CHAPTER IV

RESULTS AND DISCUSSION

With the distinguished nanosize of MNPs combined with the highly reactive elctrophilic VDM which acts as a linker for PNA to attach by using the *N*-terminus created a new approach for construction of the nanosize biomolecular detection probe. Examination whether the length of *ss aeg*PNA oligomers played an important roles for attachment themselves onto the MNPs was one of the main concern since diagnosis of DNA in cell would require *ss aeg*PNA probes with the length up to 30 mers [84-86]. Therefore, dócking of *ss aeg*PNA oligomers in such length would be inconvenient and troublesome from either primary or secondary structure of *ss aeg*PNA oligomers depending on sequence [87].

Under this study, construction of *ss aeg*PNA oligomers-MNPs probe was begun with building Fmoc-*aeg*PNA monomers containing thymine and carbazole derivatives basically prepared using HATU/2,6-lutidine and TBTU/HOBt as coupling agents, then assembling *ss aeg*PNA oligomers manually synthesized *via* solid phase synthesis on MBHA resin, subsequently calculating amount of VDM on MNPs's surface, and finally binding *ss aeg*PNA oligomers onto MNPs surface monitored by FT-IR and UV-vis spectrometry techniques. Afterward, behaviors of *aeg*PNA dimer, tetramer, hexamer, and octamer as well as behavior of *aeg*PNA probes containing different steric congestion at the *C*-terminus were observed and information from the model biomolecular probes will be used for designing the appropriate and practical *aeg*PNA oligomers-MNPs probes in the future.

Synthesis of Fmoc-*aeg*PNA monomers containing thymine and carbazole derivatives

To synthesize Fmoc-*aeg*PNA monomers, it was generally divided into three parts: 1) construction of Fmoc-*aeg*PNA hydrochloride salt **40**, 2) preparation of thymine acetic acid **44** and carbazole derivatives acetic acid **(47, 51, 53)** and

3) coupling aromatic acetic acid with Fmoc-*aeg*PNA backbone **40** to produce desired Fmoc *aeg*PNA monomers **54a-d**.

1. Construction of Fmoc-*aeg*PNA backbone hydrochloride salt (60)

Synthesis of the Fmoc *aeg*PNA backbone was first reported by Thomson et al. [77]. The procedure began with excess amount of ethylenediamine **(36)** reacted with *tert*-butyl bromoacetate **(37)** at 0 °C overnight to give monoalkylated **38**. Noticeably, *tert*-butyl bromoacetate was gradually added over a period of 5 h. in order to diminish the production of dialkylated **57** which caused the purification step become tedious (Scheme 28).

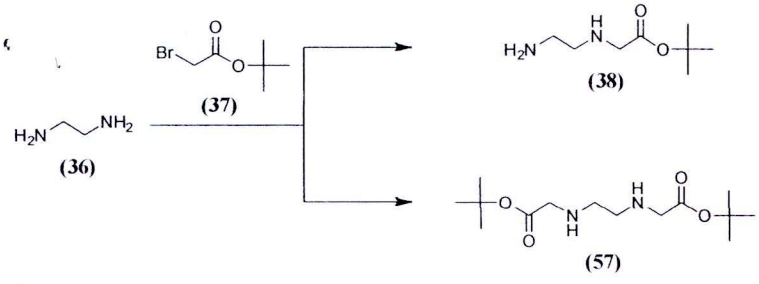

Scheme 28 Monoalkylation and dialkylation of ethylenediamine (36) with *tert*-butyl bromoacetate (37)

Next, excess ethylenediamine was removed by simply washing with water. The monoalkylation product, *tert*-butyl 2-aminoethyl glycinate **(38)**, was obtained in 65 % yield. Without further purification, **38** was subsequently reacted with *N*-(9-fluorenylmethoxycarbonyloxy)succinimide **(39)** in the presence of diisopropyl ethylamine (DIEA) to protect primary amino group with Fmoc group, a basic labile protecting group. Addition of **39** was carried out over period of 5 h. to ensure the complete protection of the primary amino group. After the reaction was ended, solvent was partially removed and the dilute hydrochloric acid was added to convert the desired product to Fmoc-*aeg*PNA backbone hydrochloride salt **40** which easily precipitate by cooling reaction mixture at -20 °C overnight in 44 % yield.

Structure of the desired product was confirmed by ^{1}H NMR technique. As shown in figure 22, chemical shift at 7.52 ppm clearly indicated the transformation of

primary amine of **35** to carbamate group. The white solid of hydrochloride salt **40** can be stored at -20 °C without decomposition over a long period of time. Under this study, **37** was orthogonally designed as backbone extender by using the base-labile Fmoc protective groups which can be selectively removed with 20 % piperidine and the acid-labile BOC groups which easily deprotected with trifluroacetic acid (TFA).

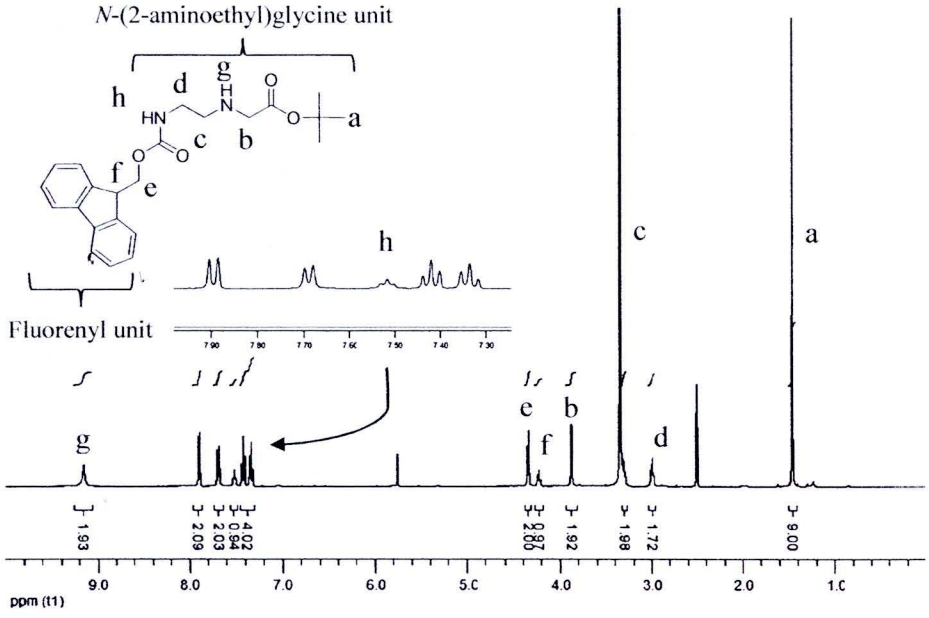

Figure 22 ^{1}H NMR Spectrum of *tert*-Butyl *N*-[2-(*N'*-9-fluorenylmethoxycarbonyl) aminoethyl] glycinate hydrochloride salt (40) ($CDCl_3$)

2. Preparation of thymine acetic acid and derivatives of carbazole acetic acid

To prepare thymine acetic acid **44** (Scheme 29), thymine was dispersed in anhydrous DMF at ambient temperature in the presence of potassium *tert*-butoxide in order to deprotonate at less steric hindrance acidic proton of thymine. Next, methyl bromoacetate **(42)** was slowly added and then stirred overnight to give thymine methyl ester **43** in 71 % yield. Subsequently, **43** underwent basic hydrolysis and followed by acidify until pH = 2 to produce desired thymine acetic acid **(44)** in 87 % yield as white solid. Spectra of ^{1}H and ^{13}C NMR of thymine acetic acid **(44)** was similar with those in previous reported by Dueholm *et al* [78].

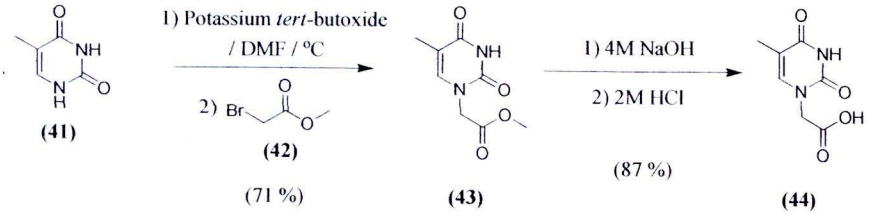

Scheme 29 Synthesis of thymine-1-yl acetic acid (44)

In addition to **44,** carbazole acetic acid **47** was also synthesized by employment similar transformation except sodium hydride was applied for the alkylation step (Scheme 30) and the total yield for two steps was 88 % yield. The final product of **47** was confirmed by ^{1}H and ^{13}C NMR and it was identical with the previous reported by Mukthung, C. [79].

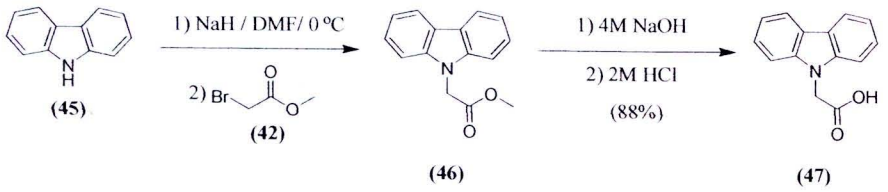

Scheme 30 Synthesis of carbazole-9-yl acetic acid (47)

To synthesize derivatives of 3,6-disubstituted carbazole acetic acid ,which could not be directly prepared from carbazole acetic acid **(47)** due to purification step of all 3,6-disubstituted carbazole acetic acid were difficult and yield were quite low. For higher yield and ease of preparation, carbazole-9-yl ethyl acetate **(48)** was employed as starting material in which easily prepared by esterification of carbazole-9-yl acetic acid **(47)** with thionyl chloride and absolute ethanol (Scheme 31) with 81 % yield [79].

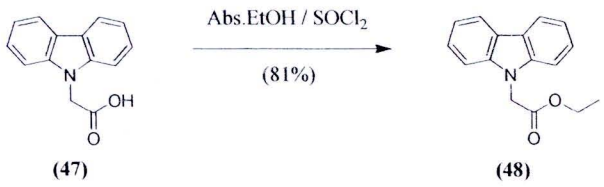

Scheme 31 Synthesis of carbazole-9-yl ethyl acetate (48)

Next, derivatives of 3,6-disubstituted carbazole acetic acid **(51, 53)** were achieved by using difference approach (Scheme 32). For example, 3, 6-dicyano carbazole-9-yl ethyl acetate **(50)** were synthesized *via* 3,6-dibromocarbazole-9-yl ethyl acetate **(49)** as intermediate by treatment of **48** with NBS as brominating reagent providing **49** in 87% yield. Then, **49** was followed by CuCN in NMP and refluxed to produce 3,6-dicyanocarbazole ester **50**. Finally, base hydrolysis was performed and 3,6-dicyanocarbazole acetic acid **(51)** was readily obtained in 86% yield [80].

To prepare 3,6-dinitrocarbazole acetic acid **(53)**, **48** was reacted with $Cu(NO_3)_2.3H_2O$, nitrating agent, in the presence of acetic anhydride to give 3,6-dinitrocarbazole ester **(52)** in high yield. After that, **52** was purified by recrystallization and column chromatography. Finally, **52** was transformed to the by acid and base hydrolysis using 4M NaOH or 4M KOH, respectively.

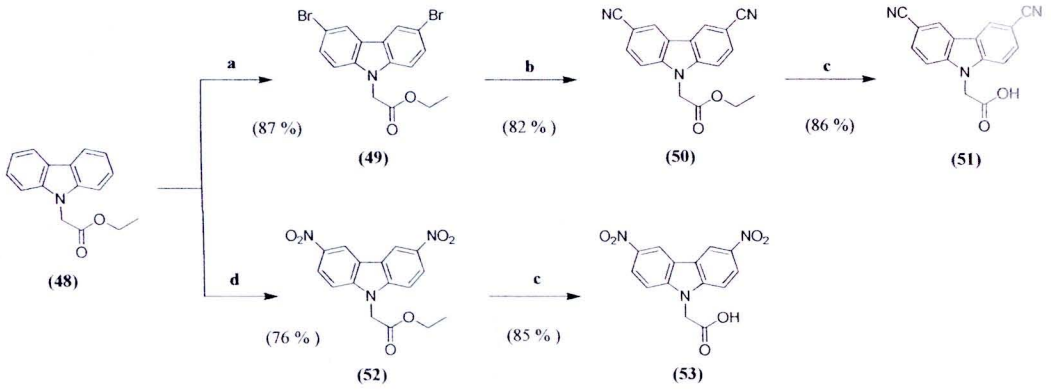

Scheme 32 Synthesis of 3,6-disubstituted carbazoles acetic acid; (a) NBS / THF / rt; (b) CuCN / NMP / reflux 4 h; (c) 4M KOH / 2M HCl; (d) $Cu(NO_3)_2.3H_2O$ / Ac_2O / HOAc / 30 °C

Derivatives of 3,6-disubstituted carbazole acetic acid were also confirmed by ^{1}H NMR spectra (Figure 23-26) the chemical shift at aromatic region clearly the splitting for disubstituted to compared in carbazole-9-yl-ethyl acetate **(48)** and compared with previous reported by Mukthung, C. [79]. Moreover, FT-IR technique was chosen to ensure the presence of nitro and cyano functional groups on the carbazole moiety. As shown in figure 30b, the signal at 2,222 cm^{-1} was appeared and it was corresponding to the cyano group (-CN stretching) for **50**. Also, signal at 1,514 and 1,335 cm^{-1} (Figure 27c) was detected and they represented an aromatic nitro group for **42** [79].

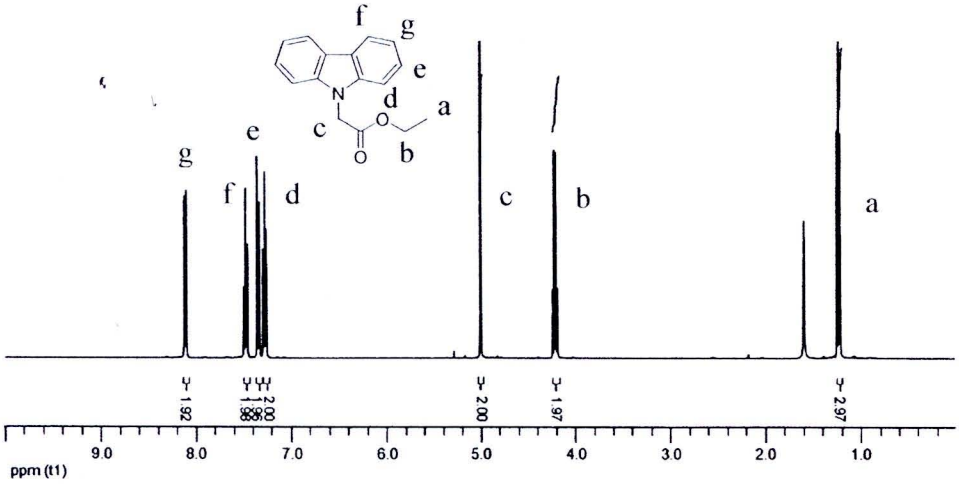

Figure 23 ^{1}H NMR Spectrum of carbazole-9-yl-ethyl acetate (48) ($CDCl_3$)

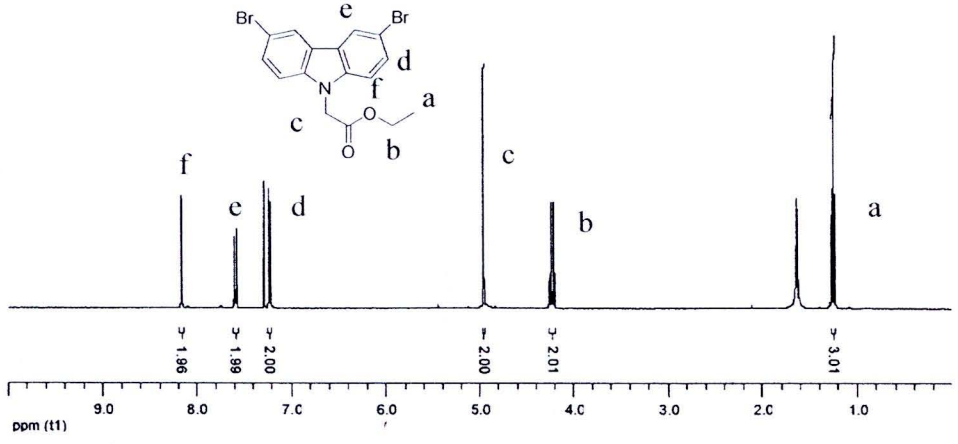

Figure 24 ^{1}H NMR Spectrum of 3,6-dibromocarbazole-9-yl-ethyl acetate (49) ($CDCl_3$)

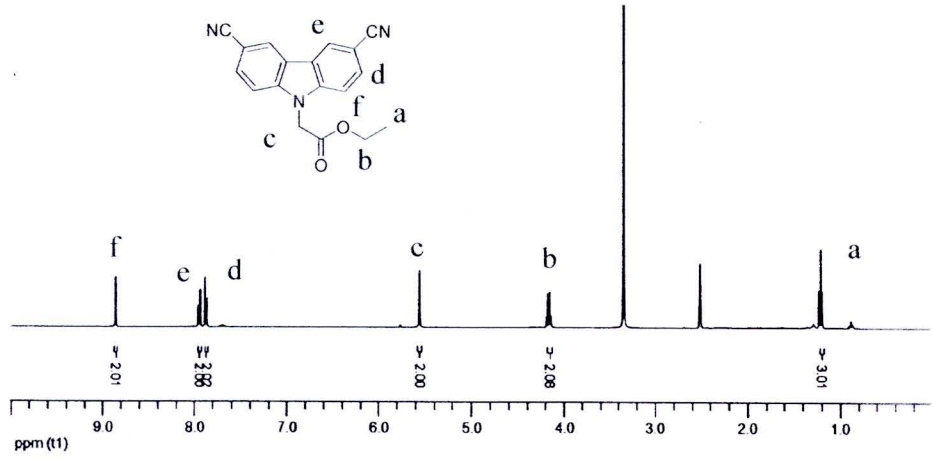

Figure 25 ^{1}H NMR Spectrum of 3,6-dicyanocarbazole-9-yl-ethyl acetate (50) (DMSO-d_6)

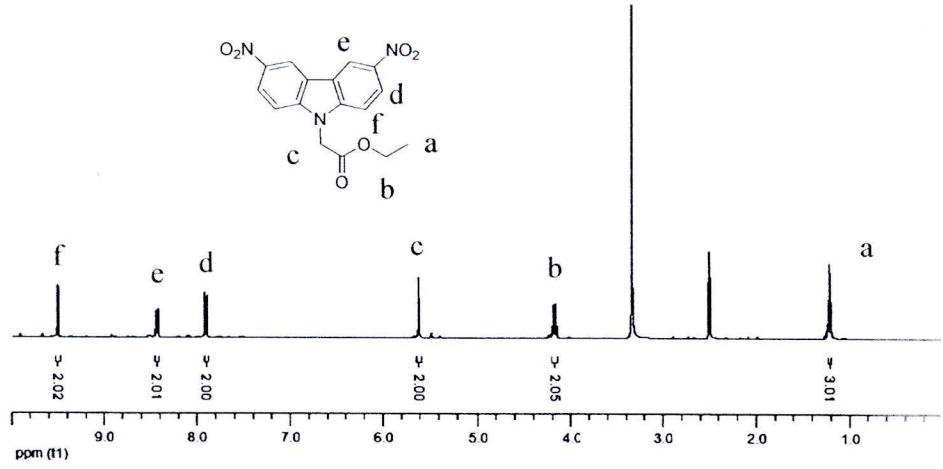

Figure 26 ^{1}H NMR Spectrum of 3,6-dinitrocarbazole-9-yl-ethyl acetate (51) (DMSO-d_6)

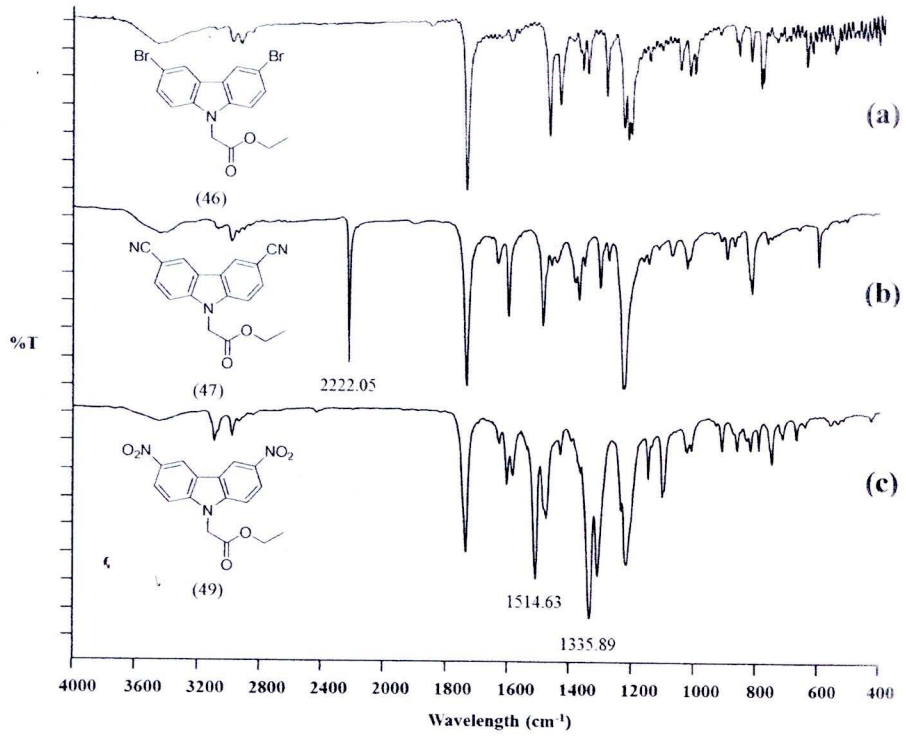

Figure 27 FT-IR Spectrum of 3,6-disubstituted carbazole-9yl-ethyl acetate (a) 3,6-dibromo, (b) 3,6-dicyano, (c) 3,6-dinitrocarbazole-9-yl-ethyl acetate

3. Preparation of Fmoc-*aeg*PNA monomers

Fmoc-*aeg*PNA monomers containing thymine, carbazole, and carbazole derivatives were conventionally prepared by employment of manual standard peptide coupling reaction [77, 79]. Generally, Fmoc-*aeg*PNA backbone **37** and 1.2 equivalents of nucleobase acetic acid **(44, 47, 51, 53)** were mixed in the presence of either 1.2 equivalents of TBTU/HOBt or HATU/2,6-lutidine and 2.5 equivalents of diisopropyl ethylamine (DIEA) in DMF (Scheme 33) producing desired Fmoc-*aeg*PNA monomers in good yield (68-81% yields). The purification was performed by column chromatography using CH_2Cl_2/MeOH as eluent. The identity of all Fmoc-*aeg*PNA monomers was confirmed by ^1H NMR and Mass spectroscopy. Interestingly, all of Fmoc- *aeg*PNA monomers were rotamer which was easily noticed from the splitting of signal in the range of 6.00-5.20 ppm for NH group to be two broad peaks compared with those in original Fmoc-*aeg*PNA backbone **40** (Figure 28). Moreover, signal to

compare pattern of CH_2 group on nucleobase indicating rotamer property for Fmoc-*aeg*PNA monomers.

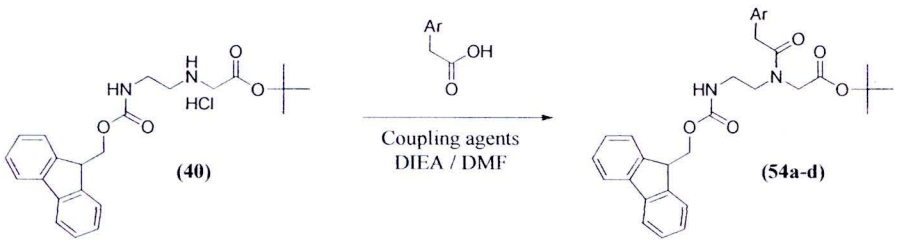

Scheme 33 Synthesis of Fmoc-*aeg*PNA monomers (54a-d)

Entry	Ar-CH_2COOH	Coupling agents	Product / Yield
44	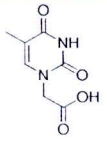	HATU/2,6-lutidine	**54a** / 78%
47	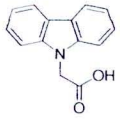	TBTU/HOBt	**54b** / 81%
51	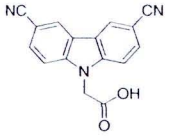	TBTU/HOBt	**54c** / 71%
53	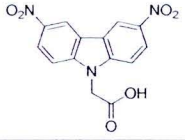	TBTU/HOBt	**54d** / 68 %

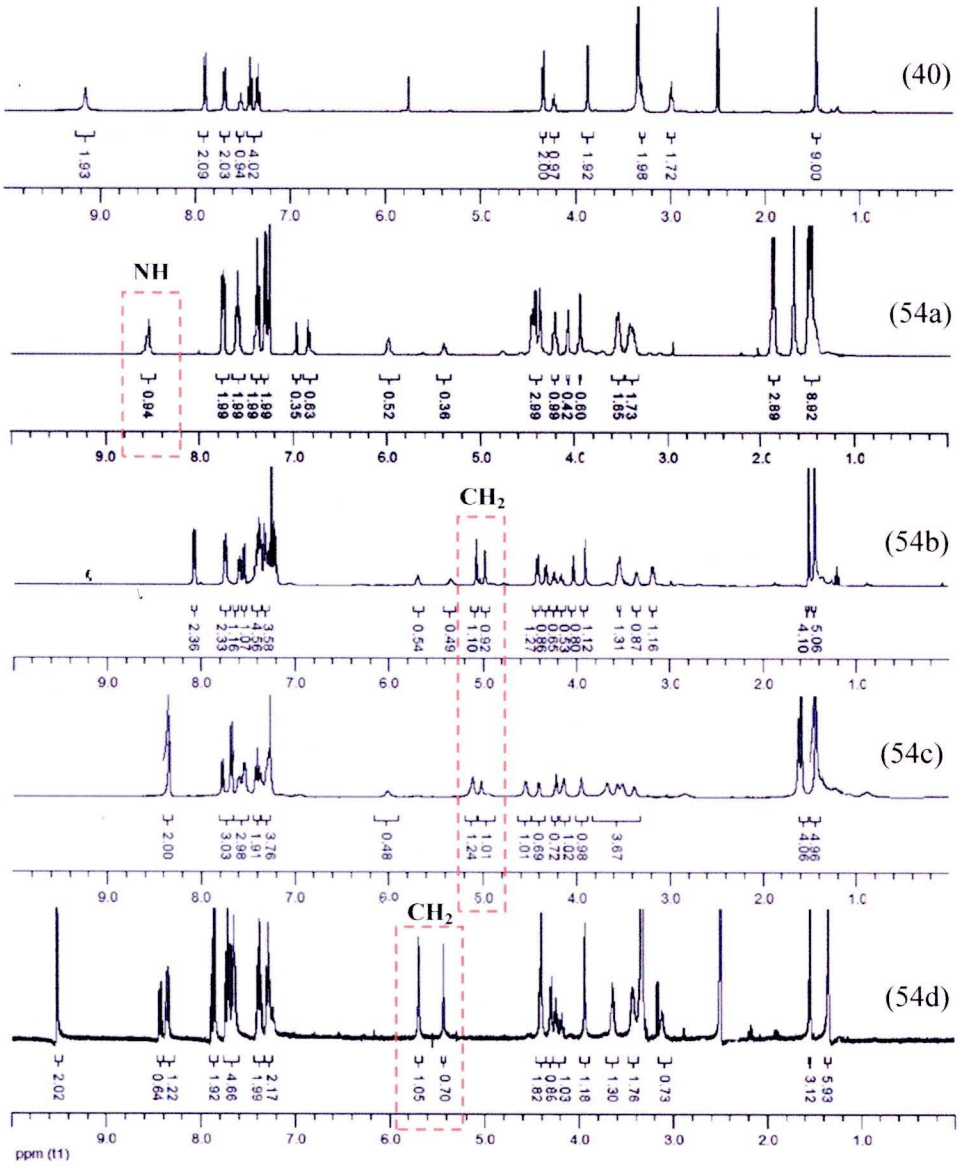

Figure 28 Overlay ^{1}H NMR spectrums of Fmoc-*aeg*PNA monomers (54a-d) to compare pattern of CH_2 group indicating rotamer property

Synthesis of *ss aeg*PNA oligomers

All *ss aeg*PNA oligomers were manually synthesized using standard Fmoc solid phase synthesis at 1 μmol scale on MBHA-resin which *aeg*PNA oligomers can easily cleave compared with other types of solid supports [84]. General procedure for preparation of *ss aeg*PNA oligomers was composed of coupling, capping, deprotection, and cleavage.

First, Fmoc-*aeg*PNA monomers were treated with trifluoroacetic acid to deblock the *C*-terminal, generating free carboxylic acids that were ready for manual coupling. Then, coupling step involves activation of Fmoc-*aeg*PNA COOH monomer with 0.2 M HATU solution (10 µL), 0.2 M DIEA and 0.3 M 2,6-lutidene solution (10 µL) for 1 min with *N*-terminus on the resin. Next, capping of the unreacted amino groups on resin by acetic anhydride ensured the desired length of *ss aeg*PNA oligomers obtained. Afterwards, deprotection of the Fmoc group at *N*-terminal growing peptide chain was performed by 20 % piperidine in anhydrous DMF at the room temperature. A synthetic single cycle consisted of about 1 hour. The coupling yields during synthesis were measured by UV monitoring at 290 nm of dibenzofulvene/piperidine (Appendix C). Finally, cleavage of the *ss aeg*PNA oligomers from the resin was successful by treatment with TFA:TFMSA:*m*-cresol (4:8:1) mixture at the room temperature. The *ss aeg*PNA oligomers were then precipitated by addition of cool diethyl ether. The suspension was centrifuged to give the crude *ss aeg*PNA oligomers as yellow fibers which were purified by reverse phase HPLC binary gradient method (Figure 29) by UV monitoring at 200, 260 and 290 nm. Noted that the column was heated to 55 °C to enhance the separation resolution and eliminate any PNA secondary structures. The purified *ss aeg*PNA oligomers were a white fiber, and were confirmed using MALDI-TOF mass spectrometry (Figure 30). As shown in the Table 4, molecular mass for target *ss aeg*PNA oligomers were in the acceptable range and this reconfirmed that target *ss aeg*PNA oligomers were successfully prepared.

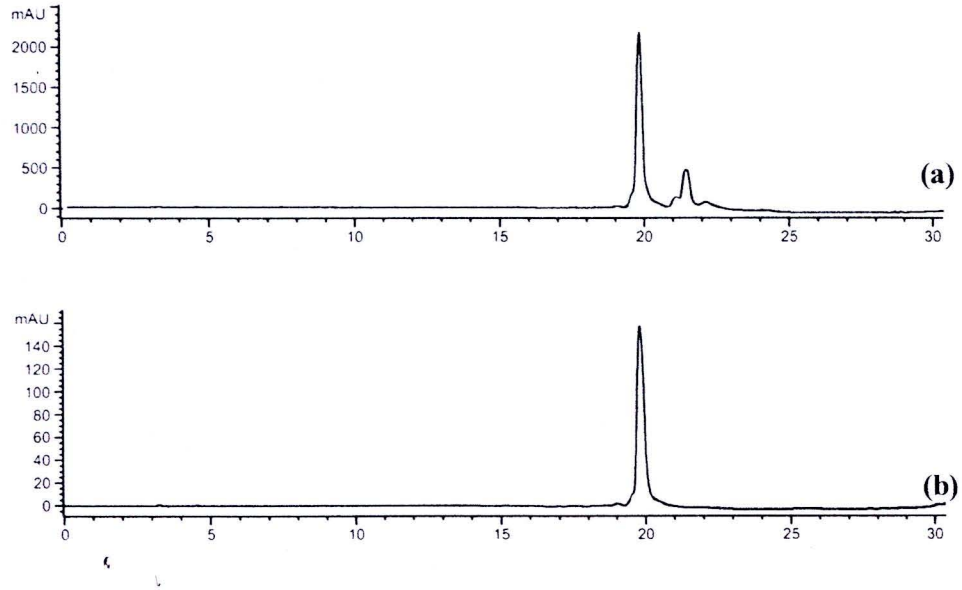

Figure 29 HPLC chromatogram of (a) crude and (b) purified PNA- T_8 (56g)

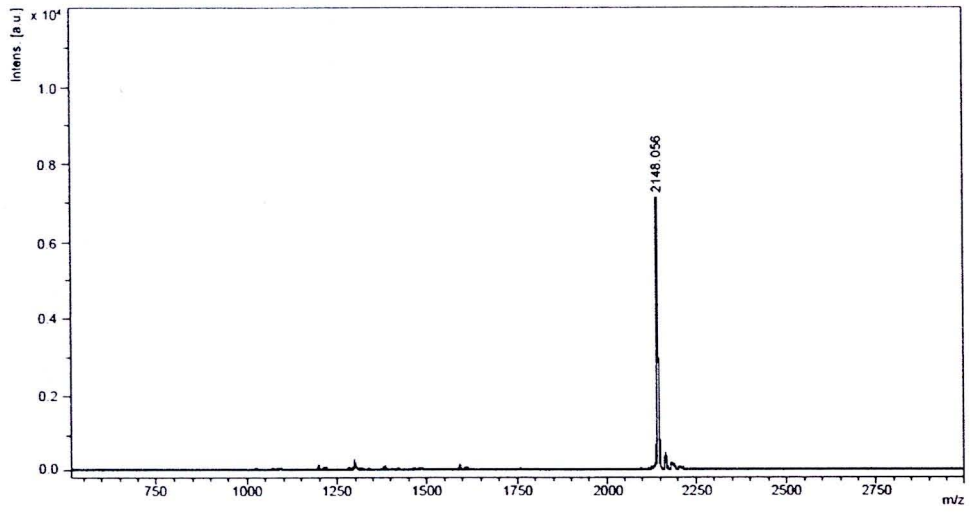

Figure 30 MALDI-TOF mass spectrum of purified PNA- T_8 (56g)

Table 4 Coupling efficiency and molecular mass of target *ss aeg*PNA oligomers (56a-g)

Code of *aeg*PNA	Coupling efficiency (%)		t_R (min)	Mass (m/z)	
	Average	Overall		Calculated	Found
T_2	97.7	95.4	7.73	549.54	549.98
T_4	98.6	94.3	12.19	1082.04	1082.52
T_6	96.2	79.4	14.92	1614.95	1615.82
TC_6	97.4	85.7	17.19	1655.64	1656.13
TCC_6	97.8	86.7	14.05	1745.64	1746.36
TNC_6	95.4	74.8	11.52	1705.66	1706.93
T_8	96.9	77.6	19.77	2147.56	2148.05

Noticeably, the longer of *ss aeg*PNA oligomers were synthesized; the lower of the overall coupling yield would normally obtain which generally found in manual coupling synthesis; even though, it was found that average efficiency for each coupling steps were more than 90 % coupling efficiency. One possibility might contribute from an intramolecular acylation of oligomers after deprotection due to the primary amine is more reactive than those of α-amino acid as shown in Scheme 34 [77].

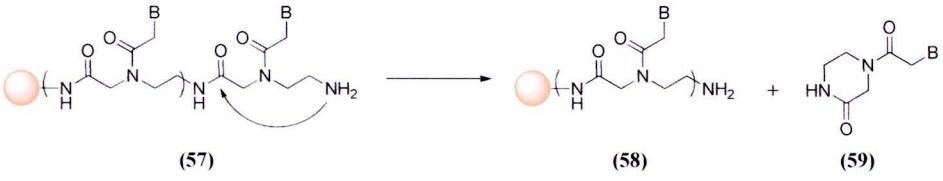

(57) (58) (59)

Scheme 34 Intramolecular acylation in synthetic *ss aeg*PNA oligomers *via* SPPS

Loading of 2-vinyl-4,4-dimethylazlactone (VDM) as electrophilic group on MNPs

VDM [66] is an azlactone heterocyclic and possess reactive electrophilic behavior toward nucleophiles including primary amines, alcohols, thiols, and peptide generally undergoes ring-opening reaction with nucleophiles. Preliminary study of VDM with water was performed and peak at 12.19 ppm and at 8.25 ppm were

appeared (Figure 31b) corresponding to OH of carboxylic acid and amide group (-NH) indicating azlactone ring was disrupted.

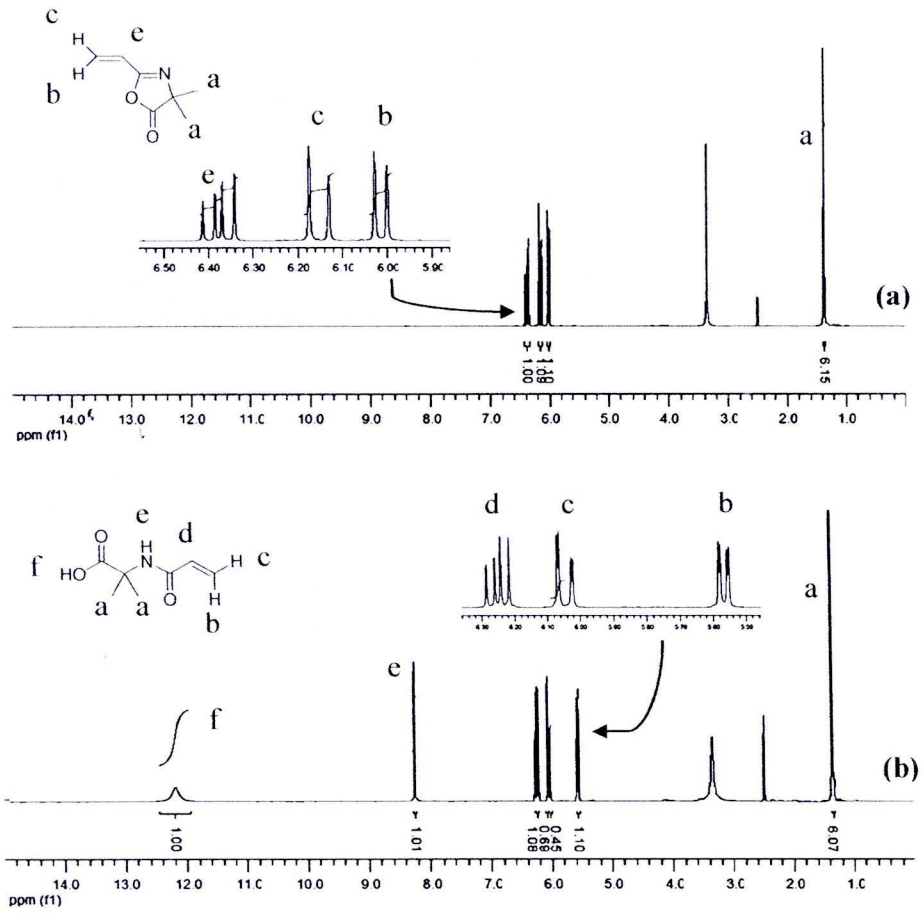

Figure 31 ^{1}H NMR spectrum of (a) VDM (b) VDM with water (DMSO-d_6)

As the benefit of that study, amount of VDM on the surface of MNPs could be indirectly calculated from amount of carboxylic acid. If amount of VDM was accurately determined, amount of *ss aeg*PNA oligomer probes would be easily predictable. To proof this idea, indirect determination of loading of VDM (mmol.g^{-1}) from carboxylic acid group was achieved by performing back-titration of MNPs with HCl solution as the titrant in which this procedure was developed by Cai *et al.* [83].

As seen in figure 32, three different intervals of conductometric back-titration curve were observed. First, the rapid descending curve followed by the interval I

corresponding to the neutralization of excess OH- ion causing a decrease of conductivity to the first minimum point, which was an increase in the volume of HCl. Second, the minimum point in interval II relating to the titration of carboxylic acid groups at the particle surface was reached. Finally, the excess of HCl solution added caused the ascending back-titration curve in the interval III.

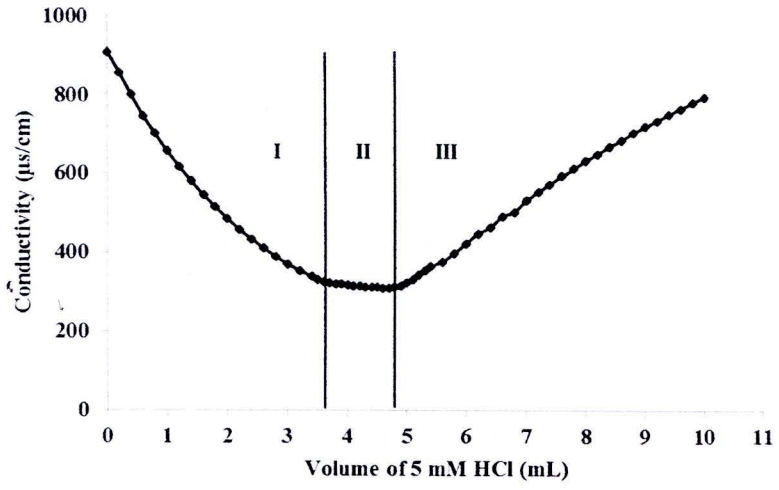

Figure 32 Conductometric back-titration curve of active site on MNPs with HCl

The equivalent point of the back-titration was determined from the difference of 5 mM HCl volume between the first and second minimum points of back-titration curve of MNPs (~1.12 mL). Therefore, the surface concentration of carboxylic acid can be calculated as follows (eq. 1):

$$Carboxylic\ acid\ (mmol.g^{-1}) = \frac{M\,\Delta V}{m} \qquad (1)$$

where, M and ΔV are the concentration of 5 mM NaOH solution and amount of 5 mM HCl solution, respectively. m is the weight of the functionalized MNPs added in the titration. According to Table 5, the concentrations of VDM on MNPs surface were 2.669 ± 0.21 mmol.g^{-1} (n=5)

Table 5 Active site on surface *via* carboxylic acid

Entry	ΔV (mL)	M (mol/L)	m (mg)	Carboxylic acid ($mmol.g^{-1}$)
1	1.10	0.005	2.1	2.619
2	1.10	0.005	2.1	2.619
3	1.20	0.005	2.2	2.727
4	1.00	0.005	2.1	2.38
5	1.20	0.005	2.0	3.00
Average	1.12	0.005	2.1	**2.669 ± 0.21** (n=5)

ΔV = amount of 5 mM HCl solution, M = concentration of 5 mM NaOH solution, m = weight of MNPs

Immobilization of *ss aeg*PNA oligomers onto the electrophilic MNPs

1. Immobilization of NH_2-*aeg*-thymine-COOH monomer onto MNPs

Before building *ss aeg*PNA oligomers-MNPs probes, preliminary investigation was conducted to observe whether the oligomers were covalently attached with VDM on surface of MNPs. To obtain the appropriate conditions, Fmoc-*aeg*-thymine-OtBu **(54a)** was selected as candidate molecule since thymine is one of the natural nucleobases that easily prepared without using any protecting groups and identification of thymine on MNPs was also achieved with simple IR technique from signal at 3007, 1150 and 900 cm^{-1} of CH_3 perpendicular rocking to the plane ($\rho^{\perp}(CH_3)$) frequencies which are distinctly separated from the C-H and N-H stretching frequencies [88].

To connect Fmoc-*aeg*-thymine-OtBu onto MNPs, Fmoc-group and *tert*-butyl group were chemically cleaved to disclose active free NH_2 group to react with VDM and to reduce steric congestion of *tert*-butyl group which might obstruct the reaction between itself and MNPs. By deprotection of both protecting groups (Appendix B), NH_2-*aeg*-thymine-COOH **(60)** was produced and its structure was proved by ^1H NMR. As shown in figure 34, signal at 1.0 ppm and 8.00-7.00 ppm were disappeared confirming both protecting groups were removed corresponding to desired unprotected thymine monomer.

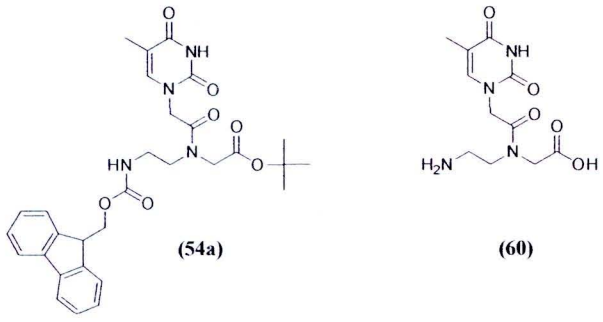

(54a) (60)

Figure 33 Structures of Fmoc-*aeg*-thymine-OtBu and NH_2-*aeg*-thymine-COOH

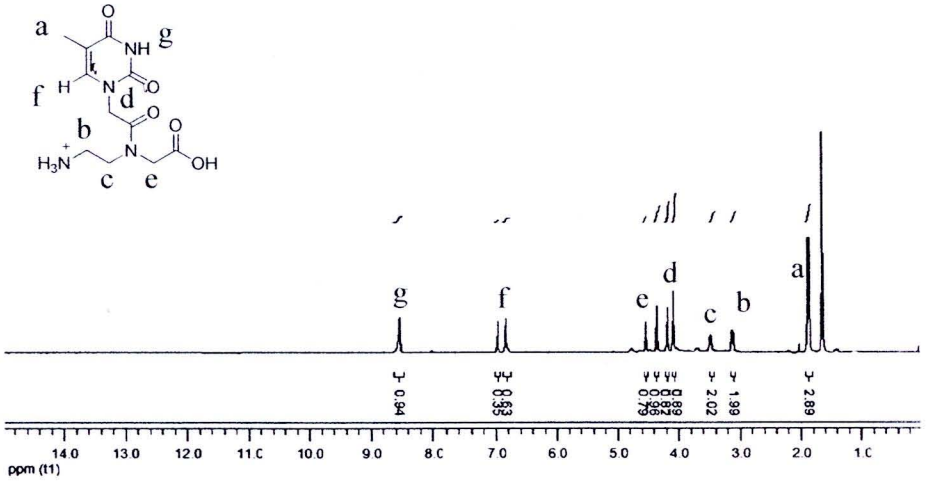

Figure 34 ^{1}H MNR spectrum of NH_2-*aeg*-Thymine-COOH salt (60) ($CDCl_3$)

Generally, both OH groups of COOH and free NH_2 groups can act as nucleophile and they were possibly interacted with VDM; however, initial study was found that only NH_2 groups underwent ring opening reaction with VDM while the OH group of COOH did not (Appendix B).

By stirring NH_2-*aeg*-thymine-COOH **(60)** in the presence of DIEA and MNPs, thymine-*aeg*PNA-MNPs complexes were obtained and they were physically removed from supernatant by external magnetic bar. Then, the thymine-*aeg*PNA-MNPs complexes was thoroughly washed with DMF : 1,4-dioxance (1:4) to remove non-specific *aeg*PNA monomer from MNPs. From the previous study, it was found that washing at least 5 times was completely removed all non-specific *aeg*PNA monomers from the desired thymine-*aeg*PNA-MNPs complexes (Figure 36).

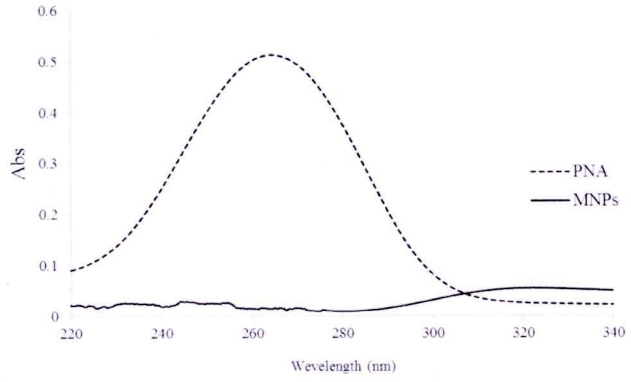

Figure 35 UV absorption of NH_2-*aeg*-thymine-COOH (60) and MNPs

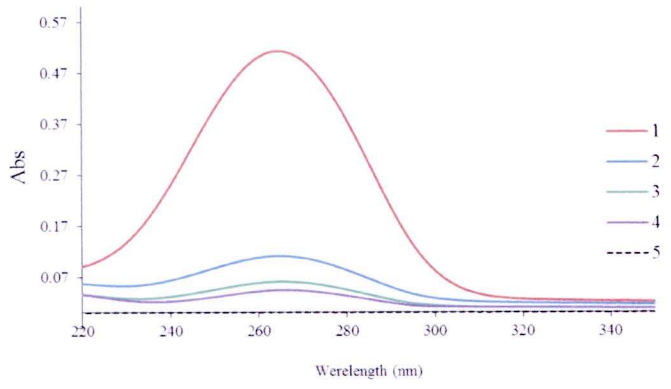

Figure 36 UV spectrum of non-specific NH_2-*aeg*-thymine-COOH (60) washing with 1,4-dioxane at 1-5 cycles

To ensure that the formation of thymine-*aeg*PNA-MNPs complexes occurred, the desired complexes were dried and were characterized by FT-IR techniques. As seen in figure 37c, signal of the CH_3 perpendicular rocking to the plane - $\rho^{\perp}(CH_3)$ at 3007, 1150 and 900 cm^{-1}, as previously mention, of thymine and Fe-O stretching at 578 cm^{-1} of MNPs were observed in which clearly indicated that thymine PNA monomer covalently connecting with MNPs.

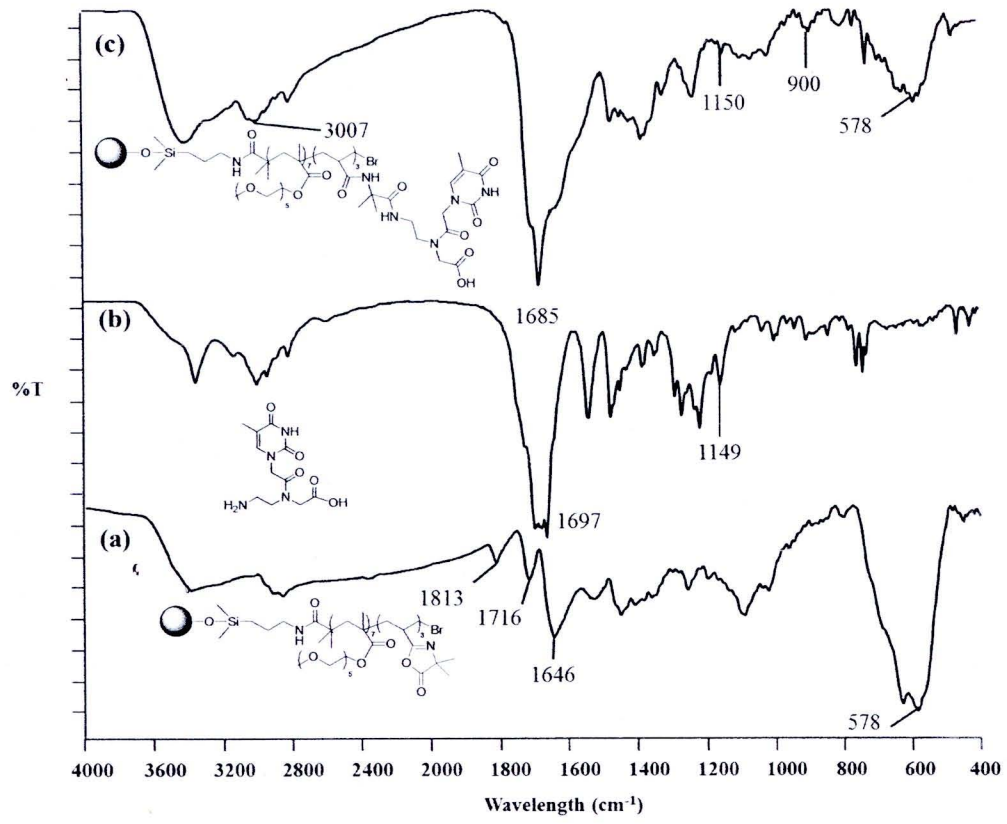

Figure 37 FT-IR spectra of (a) MNPs, (b) NH_2-*aeg*-Thymine-COOH, (c) MNPs-*aeg*PNA-T-COOH

2. Optimization for immobilization of thymine-*aeg*PNA (60) on electrophilic MNPs

Previously, it has been shown that NH_2-*aeg*-thymine-COOH **(60)** monomer covalently bonded with MNPs. To examine effect of length and steric of *ss aeg*PNA oligomers onto immobilization, exact amount of *ss aeg*PNA oligomers must be quantitated in order to compare the efficiency of attachment.

By performing kinetic study, different concentrations of thymine-*aeg*PNA monomer **(60)** were employed to react with MNPs. After thoroughly washed, unreacted thymine-*aeg*PNA monomer **(60)** can be measured by UV-vis spectrometry. Therefore, the concentration of unreacted thymine *aeg*PNA monomer can be calculated by using Beer's law (eq. 2):

$$A = \varepsilon bc \qquad (2)$$

where, The A are the absorbance of the solution at 260 nm and ε is the extinction coefficients of individual residues for thymine *aeg*PNA = 8,600 $L.mol^{-1}.cm^{-1}$. The *b* and *c* are the path length of the cell (cm) and the concentration of the solution ($mol.L^{-1}$). LOD and LOQ of thymine-*aeg*PNA monomer **(60)** was 2.44 µM and 8.12 µM (Appendix D).

As shown in figure 38, three different mole ratio of thymine-*aeg*PNA monomer:NMPs (1:1.2, 1:1.0 and 1:0.8) was used to react with MNPs (26.69 µmol, 10 mg). At 2 h., the amount of thymine-*aeg*PNA monomer on MNPs increased and it drastically increased from 4 h. to 6 h. and remains almost constant after 12 h. Therefore, this could assume that the appropriate time for immobilization of thymine-*aeg*PNA monomer was 12 h. for any concentration.

Furthermore, the appropriate mole ratio of thymine-*aeg*PNA monomer used was also determined in order to observe which ratio would produce the highest percent yield of immobilization onto MNPs. The yield of immobilization was calculated from eq. 3:

$$\text{Yield of immobilization onto MNPs} = \frac{[Thymine\ aegPNA\ monomer\ on\ MNPs]}{[Thymine\ aegPNA\ started]} \times 100 \qquad (3)$$

From figure 39, it was found that at 26.67 µmol of *aeg*PNA thymine monomer significantly provided the maximum yield of immobilization. From this data, it suggested that ratio 1:1 of MNPs and *aeg*PNA thymine monomer was the suitable concentration for immobilization.

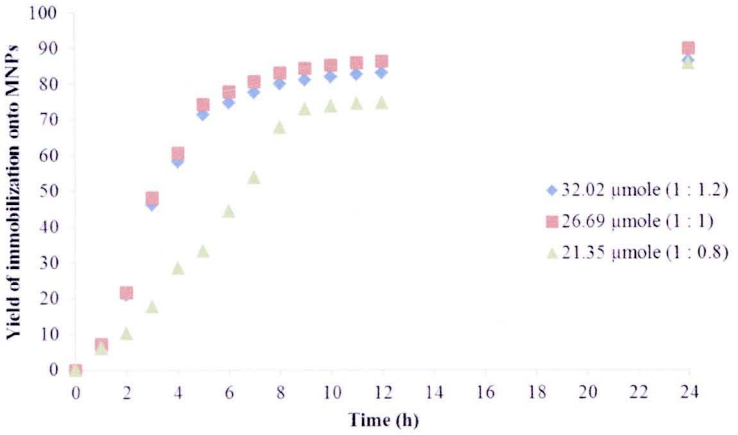

Figure 38 Kinetics study of immobilization of thymine-*aeg*PNA monomer (60) onto MNPs surface at room temperature

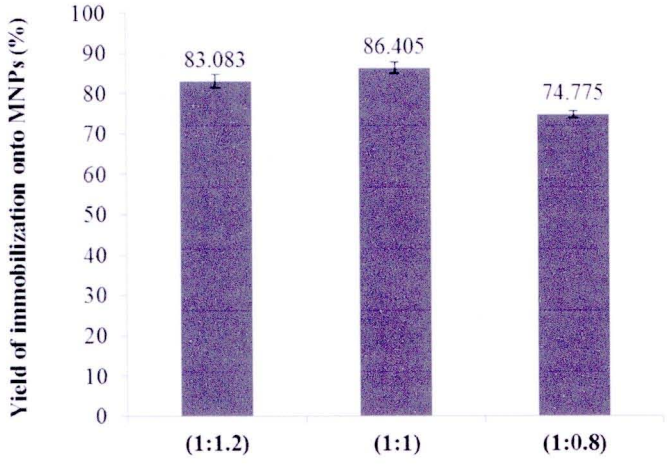

Figure 39 Optimization of thymine-*aeg*PNA monomer (60) concentrations at 12 h.

Effect of length of *ss aeg*PNA oligomers on immobilization efficiency

Length of PNA oligomers is one of the main concerns for attachment of PNAs onto MNPs. For DNA detection, normally long PNA sequence are required in order to selectively bind on the certain specific site on gene. Therefore, validation of the suitable length of PNA probe was needed for further application with actual specimens. In this study, homothymine *aeg*PNA oligomer (di, tetra, hexa and octamer)

were manually synthesized, purified by HPLC technique and desired oliogmers were confirmed by MALDI-TOF as show in Table 6.

Table 6 Sequence of homothymine *ss aeg*PNA oligomer (56a-c and 56g)

Code of *aeg*PNA	Base sequence (*N*- to *C*- terminus)	t_R (min)	Mass (m/z)	
			Calculated	Found
T_2	NH_2-TT-$CONH_2$	7.73	549.54	549.98
T_4	NH_2-TTTT-$CONH_2$	12.19	1082.04	1082.52
T_6	NH_2-TTTTTT-$CONH_2$	14.92	1614.95	1615.82
T_8	NH_2-TTTTTTTT-$CONH_2$	19.77	2147.56	2148.05

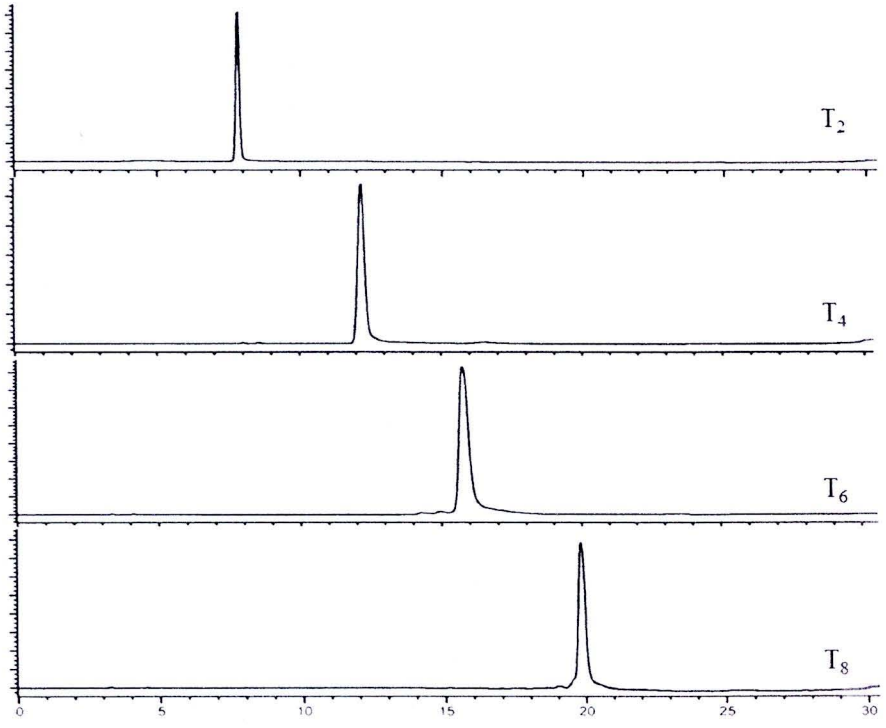

Figure 40 HPLC chromatogram of homothymine *ss aeg*PNA oligomers

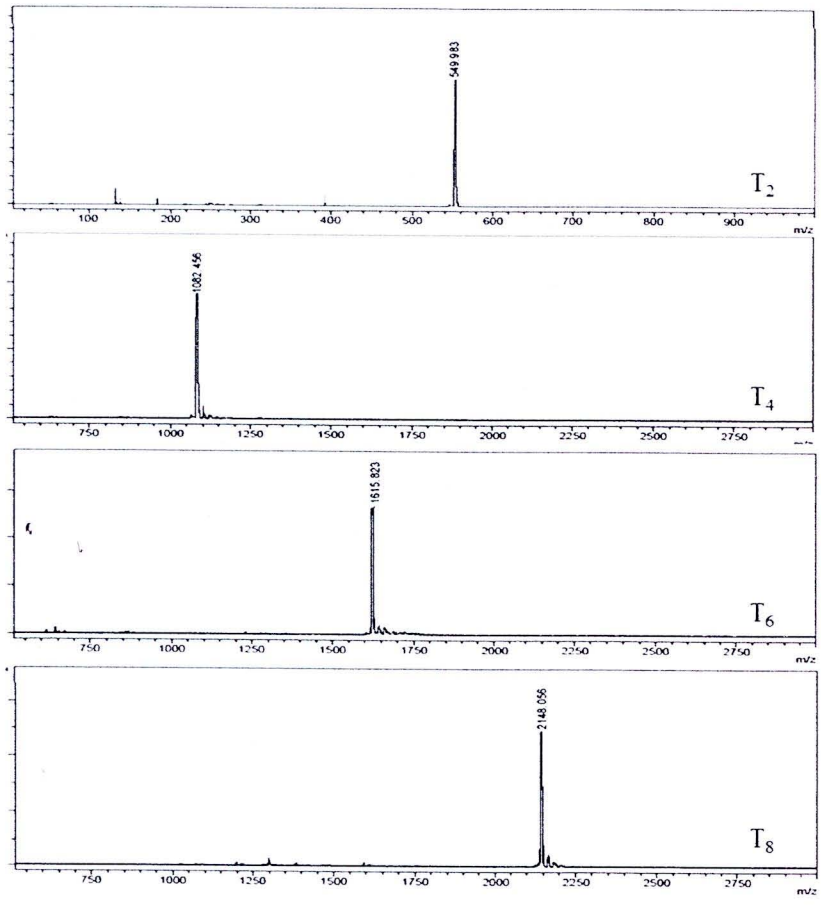

Figure 41 MALDI-TOF mass spectrums of homothymine *aeg*PNA oligomers

From previous optimization data, the immobilization between MNPs and (di, tetra, hexa and octamer) homothymine was performed at ratio 1:1 for 12 h. From figure 42, it was found that > 70 % of di, tetra, hexamer homothymine *aeg*PNA were attached on MNPs and it appeared that percent of immobilization were not significantly different. On the other hands, octamer homothymine showed only 38 % of PNA oligomers on MNPs. A drastically diminish of the immobilization in octamer, presumably due to the lowest reactivity of *aeg*PNA octamer which can be ascribed to steric hindrance from secondary structure of itself [87] and entanglement between electrophilic polymer on MNPs surface and length of octamer *aeg*PNA. However, it was found that increasing reaction time of *aeg*PNA octamer could improve the immobilization efficiency almost 10%.

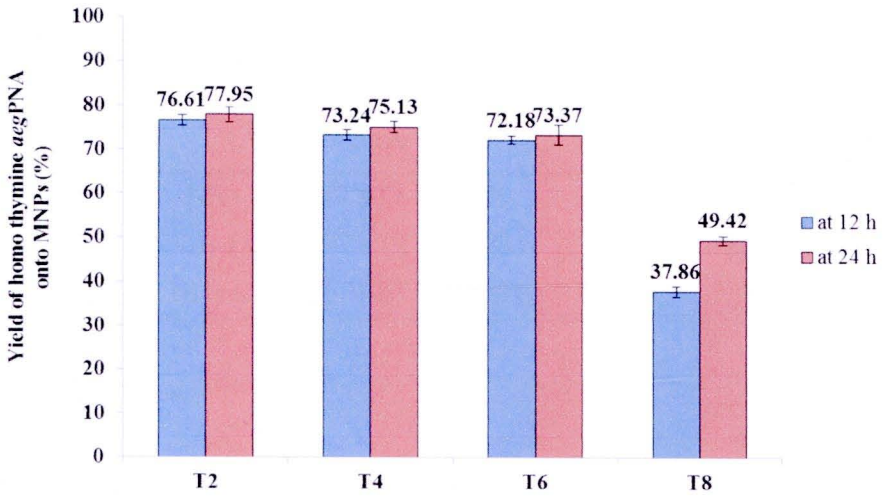

Figure 42 Effect of length of homothymine *ss aeg*PNA oligomers attach onto MNPs at room temperature

Effect of steric of *ss aeg*PNA oligomers on immobilization efficiency

To determine the SNP in actual cell, specific sequence of the target gene might not be totally elucidated and ambiguous bases could be detected; therefore, universal bases are required to incorporate against ambiguous position in order to maintain duplex formation while performing DNA analysis. Several universal bases has been reported for example, pyrene.

In this investigation, *ss aeg*PNA oligomers containing carbazole derivatives (3,6-dinitro and 3,6-dicyano carbazole derivatives) as universal bases were employed due to their high dipole moment and large surface area which might exhibit a good universal base. By varying the size and surface area of aromatic moiety, steric congestion of these universal bases can pose the effect on immobilization of themselves onto MNPs

All of *ss age*PNA hexamers containing carbazole derivatives (3,6-dinitro and 3,6-dicyano carbazole derivatives) were manually synthesized and purified by HPLC technique as shown in Table 7 and Figure 4.3.

Table 7 Sequence of ss *age*PNA hexamers containing carbazole derivatives

Code of *aeg*PNA	Base sequence (*N*- to *C*- terminus)	t_R (min)	Mass (m/z)	
			Calculated	Found
TC_6	NH_2-CBZ-TTTTT-$CONH_2$	17.19	1655.64	1656.32
TCC_6	NH_2-DCCBZ-TTTTT-$CONH_2$	14.05	1705.66	1706.41
TNC_6	NH_2-DNCBZTTTTT-$CONH_2$	11.52	1745.64	1746.28

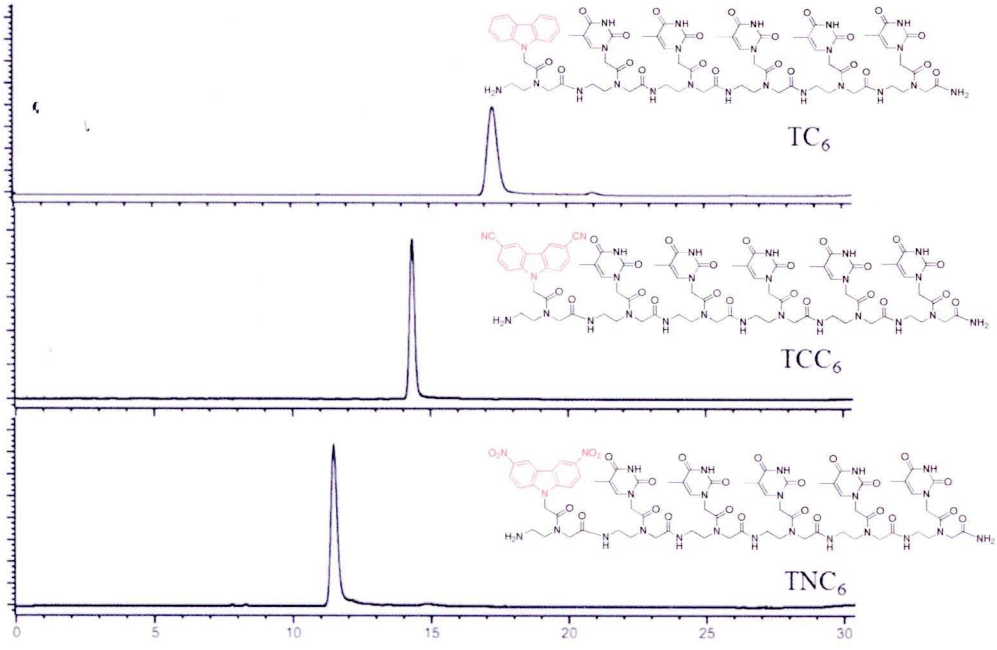

Figure 43 HPLC chromatogram of *ss aeg*PNA hexamers containing carbazole derivatives

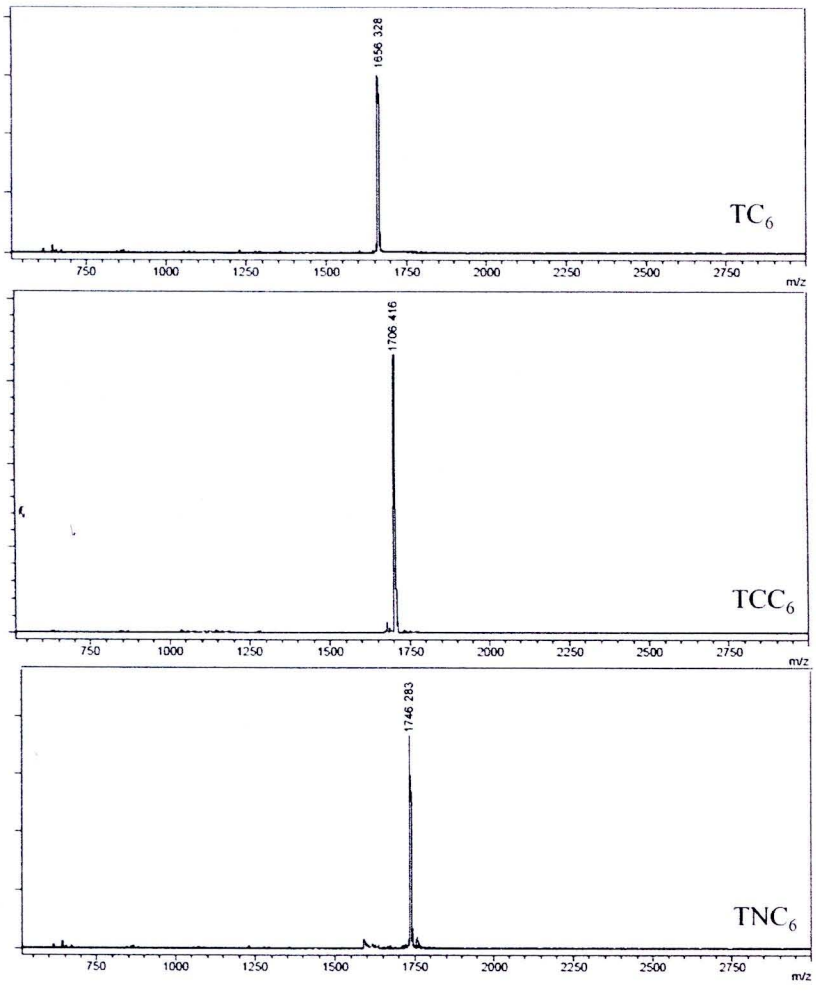

Figure 44 MALDI-TOF mass spectrums of *ss aeg*PNA hexamers containing carbazole derivatives

Next, *ss aeg*PNA hexamers containing carbazole derivatives were added to MNPs for 12 h. with ratio of 1:1 and then washed, dried and were confirmed by IR technique. The FT-IR spectra (Figure 45) showed the signal at 1152 cm^{-1} corresponding to methyl group on thymine in T_6-MNPs, TC_6-MNPs, TCC_6-MNPs complexes. Additionally, TCC_6-MNPs showed the signal at 2220 cm^{-1} corresponding to cyano group from 3,6-dicyanocarbazole moiety in Figure 4.18d; TNC_6 exhibited the signal at 1510 and 1335 cm^{-1} (Figure 45e) corresponding to nitro group on 3,6-dinitrocarbazole *aeg*PNA. Clearly, all of *ss aeg*PNA hexamers containing carbazole derivatives were successfully covalently bonded to MNPs.

For immobilization efficiency, they appeared that no significant difference for attachment of *ss aeg*PNA hexamers containing universal bases regardless of size and steric congestion at the *N*-terminus (Figure 4.6) although the reaction was change from 12 h to 24 h. This indicated that incorporated of universal bases at the end chain was feasible. However, steric volume could confer significantly effect in case of large surface area molecule incorporated with sequence such as pyrene as well as the position of universal bases located in sequence such as middle position.

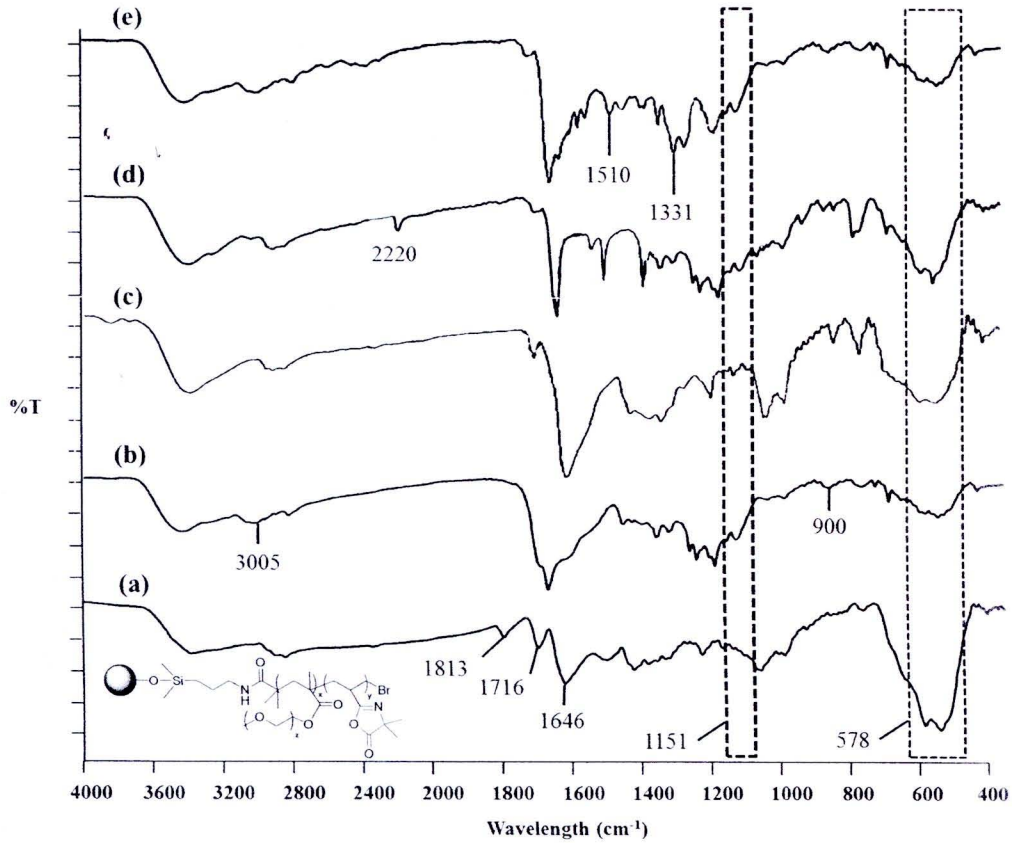

Figure 45 FT-IR spectra of (a) MNPs, (b) T_6-MNPs, (c) TC_6-MNPs, (d) TCC_6-MNPs, (e) TNC_6-MNPs complexes

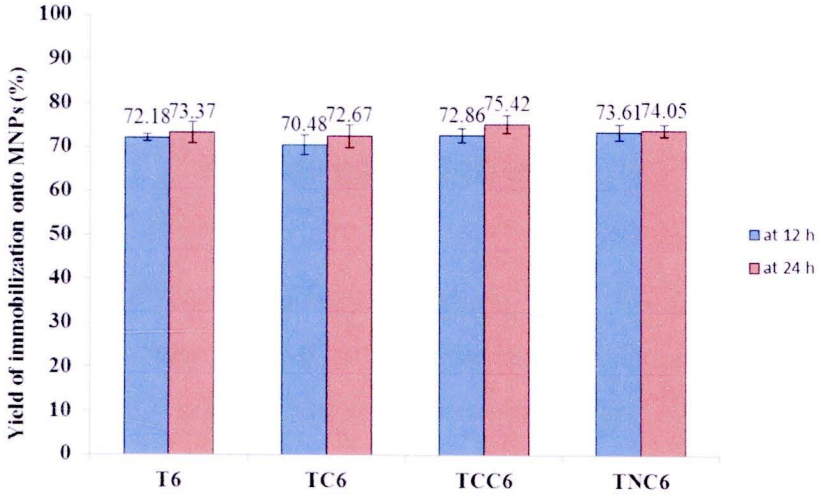

Figure 46 Effect of the steric congestion at the *N*-terminal attach onto MNP surface at room temperature